

Equation of state and melting properties of ^4He from measurements to 20 kbar

R. L. Mills, D. H. Liebenberg, and J. C. Bronson

University of California, Los Alamos Scientific Laboratory, Los Alamos, New Mexico 87545

(Received 10 December 1979)

We measured simultaneously the pressure, volume, temperature, and ultrasonic longitudinal velocity in fluid ^4He from 75 to 300 K and 2 to 20 kbar. The data were fitted to a Benedict-type equation of state from which various thermodynamic quantities were calculated. From 75 to 97 K the measurements extended into the solid region, yielding values of the melting properties and new constants for the Simon melting equation. We used the Lindemann relation to determine a Debye temperature from which the ultrasonic transverse velocity of solid ^4He was estimated. The melting entropy was analyzed to determine the contribution due to disordering of the atoms.

I. INTRODUCTION

Helium, the second most abundant element in the universe, accounts for only a small fraction of the earth's crust, where ^4He is formed by the radioactive decay of heavy metals. Although identified in the solar spectrum in 1868, helium was first isolated on earth in 1895. The gas was liquefied in 1908 and solidified in 1926. Gaseous, liquid, and solid ^4He and its lighter isotope ^3He have been studied intensively for the past 30 years to help test and refine the concepts of quantum statistical mechanics.

The industrial use of helium is presently quite small, but there are predictions of future large-scale applications in "high technology" where liquid helium, boiling at low pressure, might be employed to cool massive superconducting devices. At extremely high pressures and temperatures, helium appears as a product of hydrogen fusion and is of interest to astrophysicists and those working to produce thermonuclear energy. There is thus a need for helium equation-of-state data over a wide range of pressures and temperatures.

As shown by Wilson *et al.*¹ in a survey of experimental P - V - T (pressure-volume-temperature) data for helium, the low-pressure and low-temperature regions have been rather thoroughly investigated. At high pressures and temperatures, however, the data are spotty and often of low accuracy.

McCarty² made a critical evaluation of the thermophysical properties of fluid (gaseous and liquid) ^4He and presented calculated values in tabular form up to $T = 1500$ K and $P = 1$ kbar (1 kbar = 0.1 GPa). Bilevich and Pitaevskaya³ measured the density of fluid helium to 3 kbar at elevated temperatures and used their earlier ultrasonic data⁴ to calculate the heat-capacity ratio. The ultrasonic velocity in fluid

^4He was measured at 298.2 K by Vereshchagin *et al.*⁵ up to 3.5 kbar and by Nishitake and Hanayama⁶ up to 10 kbar. Fluid compressibility measurements were made by Tsiklis *et al.*⁷ to 7 kbar, still considerably below the 15-kbar pressure attained by Bridgman^{8,9} in his relatively crude, pioneering work on helium.

In 1959 the melting properties of ^4He and ^3He were measured up to 3.5 kbar by Grilly and Mills¹⁰ who discussed the earlier melting-curve data of others. Subsequently Crawford and Daniels¹¹ determined the melting curve to 10 kbar and Langer¹² measured one melting point at 14.14 kbar and 77.3 K. Very recently Pinceaux and Besson¹³ reported the melting pressure of ^4He to be 115 kbar at 297 K from observations made in a diamond-anvil cell.

Both helium isotopes solidify in three crystal forms^{14,15}: body-centered cubic (bcc), hexagonal closest packed (hcp), and cubic closest packed (ccp), with the ccp phase occurring at the highest temperatures and pressures. The first high-pressure studies of solid ^4He and ^3He were made by Stewart^{16,17} to measure the relative molar volume of the hcp form up to 20 kbar at 4 K. Spain and Segall¹⁸ combined existing data on solid ^4He to devise an equation of state which they extrapolated to 20 kbar for use as a pressure scale in experiments where solid helium might serve as a pressurizing agent. The large plasticity of solid helium was demonstrated by Suzuki¹⁹ who forced a steel ball through constrained solid and by Sanders *et al.*²⁰ who measured the deformation of free-standing crystals. We have suggested^{21,22} that solid ^4He would be an ideal, low- Z , highly plastic, inert, pressure medium for squeezing other samples in diamond cells.

We present measurements of P , V , T , and ultrasonic velocity u made on fluid and solid ^4He over the range $75 < T < 300$ K and $2 < P < 20$ kbar. A preliminary account of the work has already been given.²³

II. EXPERIMENTAL

The belted-anvil piston-cylinder apparatus and the experimental procedure used in the present study have been described in previous articles.²⁴⁻²⁹ Briefly, a supported tungsten-carbide cylinder 0.64-cm i.d. was filled with a known charge of helium gas at room temperature, whereupon a tungsten-carbide piston was pushed with a hydraulic press into the cylinder past the filling line to isolate and compress the sample. The piston-cylinder apparatus was then held at some constant temperature while the relative volume and ultrasonic velocity of helium were determined as a function of increasing and decreasing pressure.

Pressures were measured with a free-piston gauge in the hydraulic system of the press. Volumes were calculated from dial-gauge readings of the piston position. And temperatures were determined from calibrated thermocouples located near the top and bottom of the cylinder. We made simultaneous measurements of ultrasonic velocity u by timing both 10- and 30-MHz sound pulses over a fixed path in the sample and observed no dispersion effects.

Transitions into the solid phase were carried out slowly to insure that conditions remained near equilibrium. Our helium gas contained about 30-ppm impurities, almost all of which was neon. The experimental error in P and T was around 0.3%, while that in V ranged from 0.2% at low P and high T to about 0.5% at high P and low T . The error in u was about 0.4% overall and was less at higher densities where there was better acoustic impedance matching in the ultrasonic cell.

III. RESULTS

A. Data set

Experimental values of the molar volume of helium were needed to determine the initial quantity of gas in our cell at each filling. We found the room-

temperature measurements of McCarty,² Wiebe *et al.*,³⁰ and Biggs and Howard³¹ to be highly consistent, disagreeing by only $\pm 0.1\%$ at their highest pressure of 1 kbar. In contrast, the molar volumes of Tsiklis *et al.*⁷ are 1% higher and those of Bilevich and Pitaevskaya,³ extrapolated from higher temperatures, are 0.6% lower. We therefore used the data of Refs. 2, 30, and 31 to determine a cell loading at 295.5 K and 0.75 kbar from which pressure a compression was made to 3 kbar. Based on values of V from this run, a second loading was made at 1.4 kbar and pressurized to 10 kbar. All subsequent fillings were normalized to molar volumes from these two experiments.

We made measurements along ten isotherms, spaced about 20 K apart, between room temperature and liquid-nitrogen temperature. In addition, nine isotherms were investigated between 295.1 and 298.7 K and two were measured at 75.2 K, giving a total of 670 sets³² of P , V , T , and u .

The isothermal sets of $u_T(P)$ and $V_T(P)$ for helium were checked for computational errors by fitting them to an expression of the form $u_T, V_T = aP^b$. The exponent b was about $\frac{1}{3}$ for u_T and $-\frac{1}{3}$ for V_T , making the product of ultrasonic velocity and molar volume almost independent of pressure along an isotherm. This behavior was found also for hydrogen²⁷ and deuterium²⁸ and, as discussed previously,³³ is contrary to Rao's law for liquids and to the free-volume model.

B. Equation of state

When independent values of the ultrasonic velocity u are combined with pressure-volume-temperature data, the system becomes overdefined in the sense that u is already derivable from the P - V - T relationship

$$\frac{1}{u} = \frac{M^{1/2}}{V} \left\{ - \left(\frac{\partial V}{\partial P} \right)_T - T \left[\left(\frac{\partial V}{\partial T} \right)_P \right]^2 / \left[C_{p_0}(T) - T \int_{p_0}^P \left(\frac{\partial^2 V}{\partial T^2} \right)_p dP \right] \right\}^{1/2} = g(P, T) \quad (1)$$

where M is the molecular weight and $C_{p_0}(T)$ is the heat capacity at some normalizing low pressure P_0 , and is a function of T only. Since u in Eq. (1) depends on derivatives of the molar volume with respect to pressure and temperature, ultrasonic data have an important influence in shaping and refining an equation of state (EOS).

For an EOS explicit in V ,

$$V = f(P, T) \quad (2)$$

it is fairly easy to combine u with the usual variables P , V , and T to evaluate the parameters in $f(P, T)$. This can be done self-consistently by employing a double-process least-squares fit in which the sum

$$s = \sum_n [V_{\text{expt}} - f(P, T)]^2 + \sum_n \left(\frac{1}{u_{\text{expt}}} - g(P, T) \right)^2 \quad (3)$$

is minimized for n sets of P , V , T , and u experimen-

tal data points.

We chose as our form of Eq. (2) the empirical EOS,

$$V = \sum_{m=1}^3 \sum_{n=-2}^2 A_{nm} T^{n/2} P^{-m/3} = f(P, T) \quad (4)$$

introduced by Benedict³⁴ who simplified the equation to

$$\begin{aligned} V = & (A_{-1,1} T^{-1/2} + A_{0,1} + A_{2,1} T) P^{-1/3} \\ & + (A_{0,2} + A_{2,2} T) P^{-2/3} \\ & + (A_{-2,3} T^{-1} + A_{-1,3} T^{-1/2} + A_{0,3} + A_{2,3} T) P^{-1} \quad (5) \end{aligned}$$

by eliminating the six least important terms. Before we could fit our P - V - T data to Eq. (5), we had to evaluate $C_{p_0}(T)$ in Eq. (1) at our lowest experimental pressure $P_0 = 2$ kbar. Unfortunately values of the constant-pressure heat capacity for ${}^4\text{He}$ are known² only up to 1 kbar over the range 75–300 K. Although the C_p isotherms are highly irregular, we were able to make graphical extrapolations up to 2 kbar with estimated errors no larger than a few percent. The resulting values of $C_{p_0}(T)$ at $P_0 = 2$ kbar

were fitted to a polynomial in T giving (in J/mole K)

$$\begin{aligned} C_{p_0} = & 0.073960 T - 3.8754 T^{1/2} + 91.968 \\ & - 523.81 T^{-1/2} + 1299.1 T^{-1} \quad (6) \end{aligned}$$

which is valid over the range $75 < T < 300$ K.

Using Eqs. (1), (3), (5), and (6) and our 670-point data set,³² we determined the EOS of fluid ${}^4\text{He}$ to be (in cm^3/mole)

$$\begin{aligned} V = & (22.575 + 0.0064655 T - 7.2645 T^{-1/2}) P^{-1/3} \\ & + (-12.483 - 0.024549 T) P^{-2/3} \\ & + (1.0596 + 0.10604 T - 19.641 T^{-1/2} \\ & + 189.84 T^{-1}) P^{-1} \quad (7) \end{aligned}$$

in the region $2 < P < 20$ kbar and $75 < T < 300$ K. In Figs. 1 and 2 we show V and u , respectively, calculated from Eq. (7) and plotted versus pressure along five isotherms at 100, 150, 200, 250, and 300 K.

Figure 3 is a deviation plot of $(V_{\text{expt}} - V_{\text{calc}})/V_{\text{calc}}$ in percentage as a function of pressure at different temperatures to show the quality of fit. A similar plot of $(u_{\text{expt}} - u_{\text{calc}})/u_{\text{calc}}$ is shown in Fig. 4. For the 370 selected points in Figs. 3 and 4, the average deviation in V is $\pm 0.3\%$ and that in u is $\pm 0.5\%$, which approximates our experimental error.

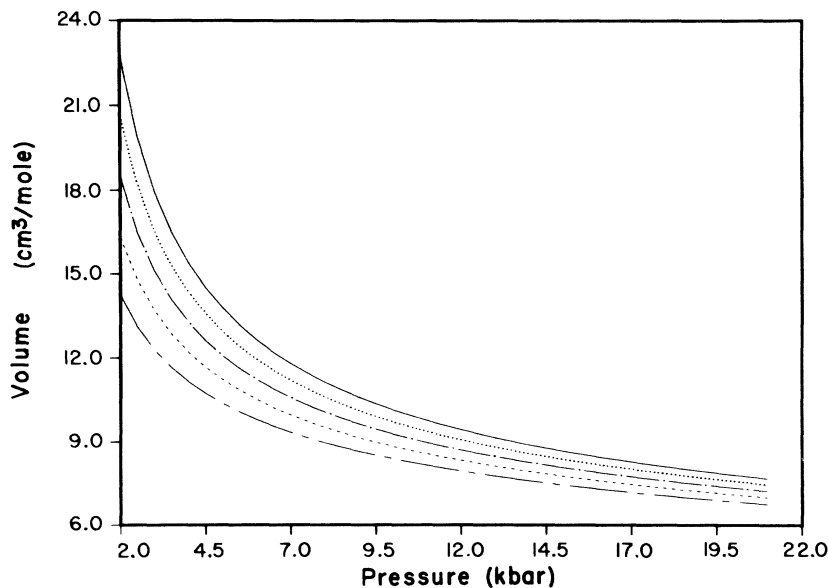


FIG. 1. Molar volume of fluid ${}^4\text{He}$ as a function of pressure along five isotherms computed from Eq. (7). Solid line, 300 K; dotted line, 250 K; chain-dot line, 200 K; short-dash line, 150 K; chain-dash line, 100 K.

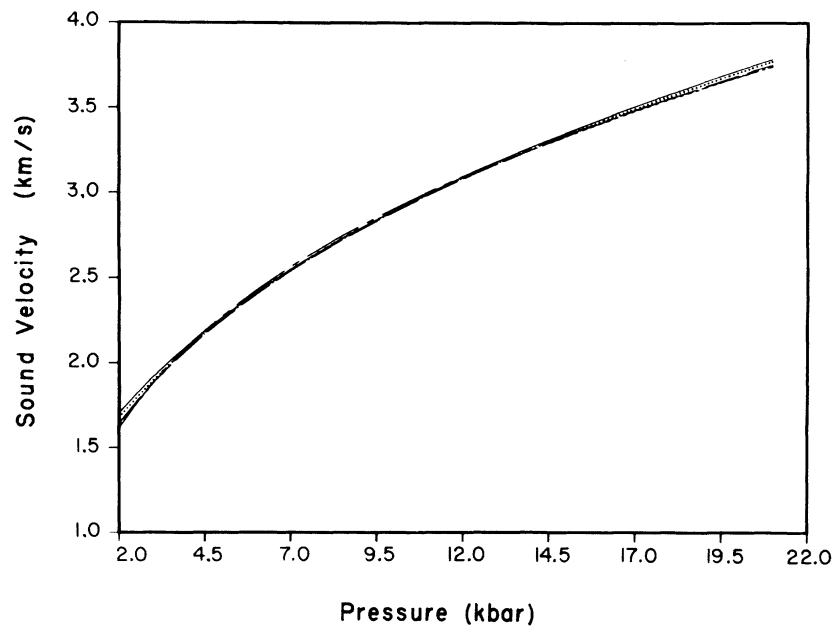


FIG. 2. Ultrasonic velocity in fluid ^4He as a function of pressure along five isotherms computed from Eqs. (1), (6), and (7). Solid line, 300 K; dotted line, 250 K; chain-dot line 200 K; short-dash line, 150 K; chain-dash line, 100 K.

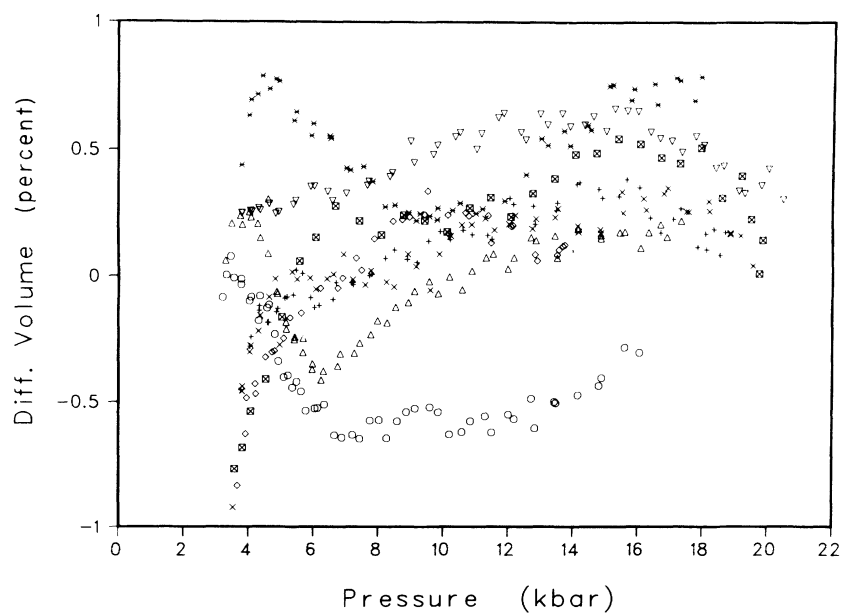


FIG. 3. Percent deviation of measured molar volumes from those calculated from Eq. (7). About 370 points for ^4He are shown. \circ , $T = 295$ K; $*$, $T = 287$ K; Δ , $T = 273$ K; $+$, $T = 249$ K; \times , $T = 201$ K; ∇ , $T = 152$ K; \boxtimes , $T = 97$ K; \diamond , $T = 75$ K.

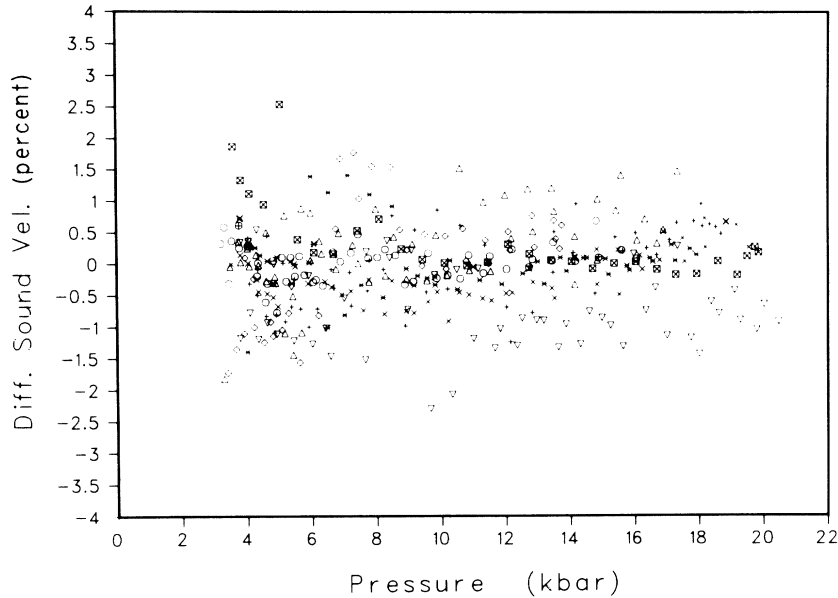


FIG. 4. Percent deviation of measured ultrasonic velocities from those calculated from Eqs. (1), (6), and (7). About 370 points for ^4He are shown. \circ , $T = 295$ K; $*$, $T = 287$ K; Δ , $T = 273$ K; $+$, $T = 249$ K; \times , $T = 201$ K; ∇ , $T = 152$ K; \boxtimes , $T = 97$ K; \diamond , $T = 75$ K.

C. Melting properties

We observed the freezing and melting of helium in four experiments, two near 75 K and two near 95 K, and list the results in Table I. The melting pressure P_m , fluid volume V_f , solid volume V_s , and volume change on melting $\Delta V_m = V_f - V_s$ were measured in all runs, but the ultrasonic longitudinal velocity u_l in solid helium was observed only at 75.22 K. Near 75 K all of the experimental melting properties are somewhat more accurate because the cell was bathed in boiling liquid nitrogen, giving good temperature control. Even so, the error in P_m , V_f , and V_s was

0.5%, while that in u_l was 1%, and the error in ΔV_m approached 10%.

We combined the melting points of Table I with those measured by Grilly and Mills¹⁰ from 1 to 3.5 kbar and by Crawford and Daniels¹¹ from 1 to 10 kbar in a least-squares fit to a Simon-type equation to obtain (in kbar)

$$P_m = -0.008112 + 0.01691 T_m^{1.5550}, \quad (8)$$

for melting pressures P_m from 1 to 20 kbar and melting temperatures T_m from 14 to 97 K. Similarly, values of the volume change on melting ΔV_m from

TABLE I. Measured values of T_m , P_m , V_s , ΔV_m , and u_l for solid helium along the melting curve. Calculated values include the Debye temperature Θ_D , the Grüneisen parameter γ , the ultrasonic transverse velocity u_t , the adiabatic compressibility coefficient χ_s , and the adiabatic Poisson ratio σ_s , as discussed in the text.

T_m (K)	P_m (kbar)	V_s (cm ³ /mole)	ΔV_m (cm ³ /mole)	u_l (km/s)	Θ_D (K)	γ	u_t (km/s)	χ_s (kbar ⁻¹)	σ_s
75.19	13.98	7.146	0.255	...	261	1.7
75.22	14.11	7.168	0.260	3.54	261	1.7	1.79	0.022	0.33
93.6	19.55	6.58	0.23	...	299	1.7
97.2	20.85	6.53	0.21	...	306	1.7

Table I, augmented by the data of Grilly and Mills,¹⁰ were used to derive the empirical expression (in cm^3/mole)

$$\Delta V_m = 0.6640(P_m + 0.1604)^{-0.3569} \quad (9)$$

for P_m from 1 to 20 kbar. Equation (8) reproduces the experimental melting pressures in Table I with an average deviation of ± 0.06 kbar, while Eq. (9) reproduces ΔV_m to about ± 0.01 cm^3/mole .

IV. DISCUSSION

A. Comparison with previous results

1. Molar volume of fluid

The only published molar volumes for ^4He with which we can compare our data directly are those of Tsiklis *et al.*⁷ at 293.2 K. Their volumes are generally larger than ours, deviating by +0.2% at 2 kbar and +2.0% at their maximum pressure of 7 kbar. The Tsiklis group also reported measurements at 323.2, 373.2, and 423.2 K. Between 2 and 7 kbar we find average deviations of about +1.5% from values of V extrapolated from Eq. (7) up to these three temperatures. Tsiklis *et al.*⁷ fitted their volume data along each isotherm to empirical equations which they extrapolated up to 15 kbar. At this pressure the deviations from Eq. (7) have reversed sign and are -2.4% at 293.2 K and -5.0% at 423.2 K. Unfortunately the Tsiklis equations go to zero molar volume at pressures around 100 kbar.

Bilevich and Pitaevskaya³ measured the density of helium gravimetrically from 0.5 to 3 kbar along isotherms at 373.2, 423.2, 523.2, and 573.2 K. They gave their data in tabular, graphical, and analytical form, but inconsistencies in their presentation make it impossible to draw comparisons except at their two lowest temperatures. Along the 373.2-K isotherm, their volumes are lower than those extrapolated from Eq. (7) by -1.6% at 2 kbar and -0.9% at 3 kbar. At 423.2 K the deviations are -2.2 and +0.1% at 2 and 3 kbar, respectively.

In general Eq. (7) can be extrapolated in pressure down to 1 kbar and in temperature down to 50 K with errors in volume less than 2%. For example, extrapolated values of V have an average deviation of only $\pm 1.3\%$ from the tabulation of McCarty² at 1 kbar over the range $50 < T < 300$ K. For T decreasing below 50 K, however, isobars at $P < 3$ kbar extrapolated from Eq. (7) go through minima and rise spuriously because of an insufficient number of temperature terms.

2. Ultrasonic velocity in fluid

The ultrasonic velocity u in fluid ^4He was measured at 298.2 K by Vereshchagin *et al.*⁵ up to 3.5 kbar, by Pitaevskaya and Bilevich⁴ up to 4 kbar, and by Nishitake and Hanayama⁶ up to 10 kbar. In the region of overlap, the velocities of Vereshchagin *et al.*⁵ agree within their stated error of 2% with those reported here. The Pitaevskaya and Bilevich⁴ results are lower than ours by 2.1% at 3 kbar and 1.0% at 4 kbar, which is slightly outside the combined experimental error of 0.8%. The ultrasonic velocities of Nishitake and Hanayama,⁶ with a reported uncertainty of 3%, deviate from the present results by 1.1% at 3 kbar and 1.3% at 10 kbar. The data of Pitaevskaya and Bilevich⁴ extended from 298.2 to 473.2 K. At these higher temperatures, ultrasonic velocities extrapolated from Eq. (7) disagree by no more than 2% with those of Ref. 4 up to 4 kbar. Our extrapolated values of u at 1 kbar are several percent higher over the range 75–300 K than those computed by McCarty, who lists no uncertainty in Ref. 2.

3. Melting curve

Since we used some of the ^4He melting points from Refs. 10 and 11 along with our measurements of Table I to derive Eq. (8), melting curves from all three sources are in good agreement. However, the difference between Langer's¹² melting pressure of 14.14 ± 0.20 kbar at 77.3 K and the value 14.59 ± 0.06 kbar calculated from Eq. (8) at the same temperature is slightly outside the combined experimental errors. Similarly the Pinceaux and Besson¹³ diamond-cell measurement $P_m = 115$ kbar at $T_m = 297$ K is lower than the value $P_m = 118$ kbar extrapolated from Eq. (8). Pressure in the diamond cell was based on the ruby-fluorescence scale.³⁵ We suggest that our melting curve might be used to calibrate the ruby pressure scale, especially at temperatures below room temperature.

The molar volume of fluid helium at melting, V_f , can be computed by combining Eqs. (7) and (8). Grilly and Mills¹⁰ measured V_f up to $P_m = 3.5$ kbar ($T_m = 30.8$ K) and expressed their results in analytical form. Extrapolation of their equation to melting pressures in the range 4 to 20 kbar gives values of V_f that deviate by an average of -1.3% from the present data. The smallest disagreement, -0.6%, occurs around $P_m = 8$ kbar ($T_m = 52.4$ K) where the combined errors are apparently minimized in extrapolations of the Ref. 10 data above the experimental range and extrapolations of our data below.

By subtracting ΔV_m in Eq. (9) from V_f , one can arrive at the solid molar volume of ^4He at melting, V_s . We find that V_s computed in this way differs by an average of only +0.25% in the range $5 < P_m < 20$

kbar from the solid volumes derived by Spain and Segall.¹⁸ In their derivation, Spain and Segall¹⁸ used Stewart's^{16,17} solid molar volumes at 4 K, coupled with the Mie-Grüneisen equation of state, to calculate pressure as a function of temperature along isochores in solid ^4He .

4. Phase diagram

To demonstrate the overall consistency of our P - V - T measurements in solid and fluid helium with those of others, we show in Fig. 5 the molar volume on a logarithmic scale plotted along isobars against a linear temperature scale. The liquidus and solidus lines, that give, respectively, the fluid and solid molar volumes at melting, are shown by the steep heavy curves. The triangles represent measurements of Grilly and Mills¹⁰ up to 3.5 kbar with extrapolations of their equations to 6 kbar. Along this portion of the phase boundary, the solid molar volumes are lower than those derived by Spain and Segall¹⁸ by 1.2% at 1 kbar and 0.8% at 6 kbar. Fluid and solid

volumes at melting pressures above 6 kbar were taken from the present measurements.

The light solid lines in Fig. 5 are isobars in fluid ^4He calculated from Eq. (7). For comparison, smoothed experimental points from all of the isotherms on which Eq. (7) was based were interpolated at rounded pressures and are shown by the open circles. The crosses at 1 kbar are from McCarty² and the exes at 4 K are from Stewart.^{16,17} Shown as dashed lines are graphical extensions of the present results. All of the measurements appear to be in good agreement.

The dash-dot line in Fig. 5 is the transition curve between hcp and ccp helium reported by Dugdale and Simon,³⁶ Mills and Schuch,³⁷ and Franck.³⁸ This phase change takes place with almost zero volume change (10^{-4} cm³/mole). There is a prediction³⁹ that the transition line will eventually bend back to 0 K at a calculated pressure between 15 and 120 kbar, depending on which intermolecular potential is used and whether or not corrections are made for many-body interactions. The transition from hcp to bcc helium occurs at low pressure and a molar volume⁴⁰ of 20.9 cm³, which lies above the V scale in Fig. 5.

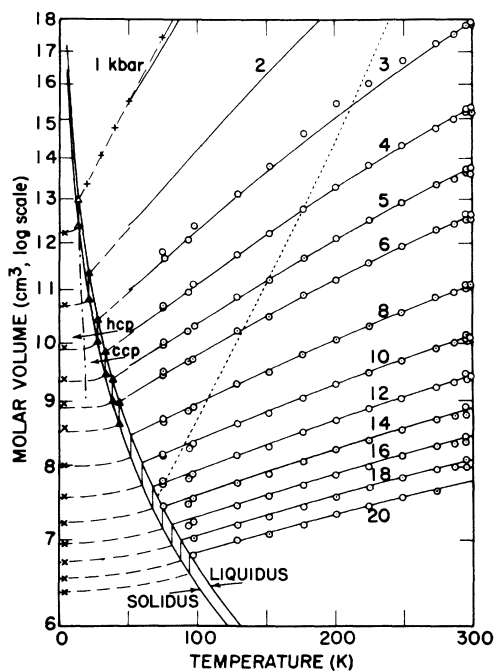


FIG. 5. Plot of $\ln V$ vs T for 13 isobars in fluid and solid ^4He . \circ , present measurements interpolated at rounded pressures; $+$, McCarty, Ref. 2; Δ , Grilly and Mills, Ref. 10; \times , Stewart, Refs. 16 and 17; heavy solid lines, melting volume of liquid and solid; light solid lines, Eq. (7); dashed lines, graphical constructions; dash-dot line, transition curve between hcp and ccp solid phases, Dugdale and Simon, Ref. 36, and Mills and Schuch, Ref. 37; dotted line, locus of $(\partial^2 V/\partial T^2)_p = 0$, Eq. (7).

B. Properties of fluid

1. Thermodynamic coefficients

The isobaric thermal expansion coefficient, $\alpha_p = V^{-1}(\partial V/\partial T)_p = (\partial \ln V/\partial T)_p$, is shown graphically as the slope of the constant-pressure lines in Fig. 5. For fluid ^4He , we computed analytical values of α_p along with the isothermal compressibility coefficient $\chi_T = -V^{-1}(\partial V/\partial T)_p$ by differentiating Eq. (7). Tabulated results can be obtained from the authors.⁴¹ The coefficients are well behaved even at 3 Mbar and 3000 K, where $\alpha_p = 1.4 \times 10^{-4}$ K⁻¹ and $\chi_T = 1.0 \times 10^{-4}$ kbar⁻¹. For comparison, the extrapolated values²⁸ for molecular deuterium (also mass 4) are 0.4×10^{-4} K⁻¹ and 1.1×10^{-4} kbar⁻¹, respectively, under the same extreme conditions.

2. Heat capacity

Shown in Fig. 5 as the light dotted line crossing the fluid isobars is the locus $(\partial^2 V/\partial T^2)_p = 0$, calculated from Eq. (7). This quantity is positive at temperatures below the locus and negative above. Since

$$C_p = C_{p_0}(T) - T \int_{p_0}^p \left(\frac{\partial^2 V}{\partial T^2} \right)_p dP, \quad (10)$$

the constant-pressure heat capacity decreases with increasing temperature below the dotted line and increases above. Values of C_p , calculated from Eqs.

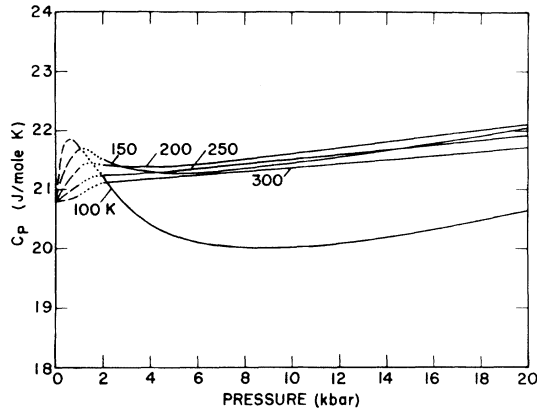


FIG. 6. Molar heat capacity C_p in fluid ${}^4\text{He}$ as a function of pressure along five isotherms. Solid lines, computed from Eqs. (6) and (7); dashed lines, data of McCarty, Ref. 2; dotted lines, smooth connecting curves.

(6), (7), and (10), are plotted along five isotherms from 100 to 300 K as the solid curves in Fig. 6. Values from McCarty's tabulation² up to 1 kbar are represented by the dashed curves, which earlier we had extended to 2 kbar to arrive at Eq. (6). The dotted-line extrapolations join smoothly with our data above 2 kbar. While our EOS cannot be expected to reproduce the complicated maxima exhibited by the low-pressure curves in Fig. 6, extrapolation of Eq. (7) to 1 kbar gives values of C_p that deviate by an average of only 1.3% from those computed by McCarty.²

We also calculated values⁴¹ of C_v from $C_v = C_p(\chi_s/\chi_T)$, where χ_s , the adiabatic compressibility coefficient, can be expressed as $\chi_s = V/Mu^2$. When extrapolated down to 1 kbar, our constant-volume heat capacities are about 7% smaller than those computed by McCarty² at temperatures from 100 to 300 K. The disagreement is just within the combined errors of 5% stated in McCarty's work and 2% in our extrapolations. Since we had, in effect, normalized our C_p data to graphical extensions of McCarty's calculations, his heat-capacity ratio $C_p/C_v = \chi_T/\chi_s$ appears to be slightly inconsistent with ours.

3. Entropy

We calculated the molar entropy of fluid helium from Eq. (7) using the equation

$$S(P, T) = S(P_0, T) - \int_{P_0}^P \left(\frac{\partial V}{\partial T} \right)_P dP, \quad (11)$$

where $S(P_0, T)$ is the absolute entropy over our experimental temperature range at our normalizing

pressure $P_0 = 2$ kbar. Again, tabulated results are available.⁴¹ To evaluate $S(P_0, T)$, we first made an S -vs- $\ln P$ fit of McCarty's² entropies, reported to a maximum pressure of 1 kbar, at 75, 100, 150, 200, 250, and 300 K. The straight-line isotherms were then extrapolated to 2 kbar and the results were fitted to (in J/mole K)

$$S_{p=2} = -58.598 + 21.314 \ln T \quad (12)$$

for $75 < T < 300$ K. Equation (12) reproduces the extrapolated entropies to $\pm 0.12\%$.

It is also possible to obtain an expression for $S_{p=2}$ over the same temperature range as that above by integrating Eq. (6) using the relationship $C_p = T(\partial S/\partial T)_p$. The result is (in J/mole K)

$$S_{p=2} = 0.07396T - 7.7508T^{1/2} + 91.968 \ln T + 1047.62T^{-1/2} - 1299.1T^{-1} - 405.69, \quad (13)$$

where the integration constant -405.69 was chosen to agree with absolute entropies extrapolated from the Ref. 2 tables. The average deviation between Eqs. (12) and (13) is only $\pm 0.06\%$ over the entire temperature range. This demonstrates that our difficult extrapolation of irregular C_p curves to give Eq. (6) at $P_0 = 2$ kbar is at least consistent with the more or less straightforward extrapolation of S . Unfortunately, reversing the procedure and trying to derive $C_{p=2}$ by differentiating $S_{p=2}$ in Eq. (12) results in the temperature-independent expression $C_{p=2} = 21.314$ J/mole K. While this value is a good average of $C_{p=2}$ over the range $100 < T < 300$ K, Eq. (12) does not contain sufficient information to give precise derivatives. The absolute entropy of fluid ${}^4\text{He}$ at melting can be calculated from Eqs. (7), (8), (11), and (12).

C. Properties of solid

1. Debye temperature

In Table I we give the Debye temperature Θ_D for solid helium at various T_m and V_s computed from the Lindemann⁴² melting equation

$$C^2 = \Theta_D^2 V_s^{2/3} M / T_m, \quad (14)$$

where C is a constant which we assume has the same value as that used in our previous work on nitrogen²⁶ and hydrogen,²⁹ namely, $C = 116 \pm 2$ cm K^{1/2} g^{1/2} mole^{5/6}. This value of the Lindemann constant agrees with $C = 117 \pm 2$ cm K^{1/2} g^{1/2} mole^{5/6} derivable from Dugdale's⁴³ measurements on solid ${}^4\text{He}$ over the range $3 < T_m < 20$ K, but disagrees with Spain and Segall's¹⁸ $C = 98.9 \pm 0.2$ cm K^{1/2} g^{1/2} mole^{5/6} computed for melting temperatures from 16 to 95 K.

Using Eqs. (7)–(9) and (14), we calculated Θ_D for melting temperatures from 50 to 100 K and found

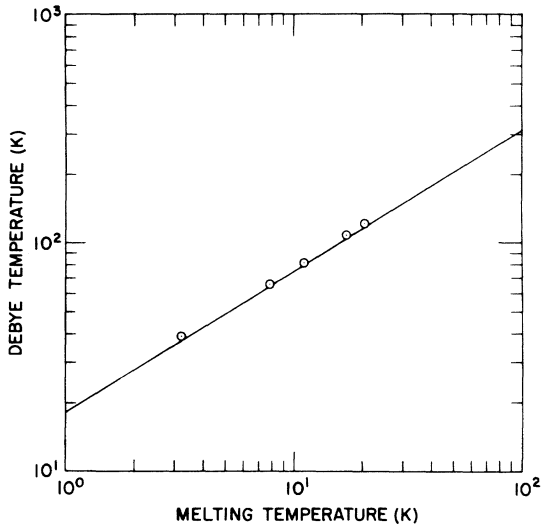


FIG. 7. Log-log plot of the Debye temperature vs melting temperature for solid ^4He . Solid line, Eq. (15); O, measurements of Dugdale, Ref. 42.

that the results could be fitted to the empirical equation (in K)

$$\Theta_D = 17.76 T_m^{0.6219} \quad (15)$$

with an average deviation of only $\pm 0.02\%$. Equation (15) is plotted as the solid line in Fig. 7 where the open circles represent the data of Dugdale.⁴² The remarkable agreement shown in Fig. 7 is further evidence that the Lindemann melting equation applies also to quantum solids such as ^4He .

2. Grüneisen parameter

The empirical relationship shown in Eq. (15) has another implication. If we define a Grüneisen parameter

$$\gamma = -d \ln \Theta_D / d \ln V_s \quad (16)$$

in terms of the Debye temperature Θ_D and solid volume V_s along the melting curve, then according to the Lindemann melting equation, Eq. (14),

$$\gamma = (3 - \frac{3}{2} d \ln T_m / d \ln \Theta_D)^{-1} \quad (17)$$

Using Eq. (15) to evaluate the right-hand side of Eq. (17), we find that the Grüneisen parameter has a constant value of 1.7, which we have entered in Table I. Furthermore, the behavior shown in Fig. 7 indicates that γ will remain fairly constant down to a melting temperature of about 3 K. For solid helium along the melting curve, Spain and Segall¹⁸ gave values of γ that varied from 2.0 at 1 kbar to 1.6 at 20

kbar, whereas Dugdale⁴³ computed a constant Grüneisen γ of 2.4 from thermal measurements on hcp ^4He and ^3He up to several kilobars. From sound velocity measurements on single crystals of ^4He up to about 0.1 kbar, Wanner and Franck⁴⁴ obtained a Grüneisen γ for longitudinal phonons of 3.0 which is comparable to the values 2.9 and 3.3 reported by Wanner and Meyer⁴⁵ for solid H_2 and D_2 , respectively, in their ultrasonic study up to 0.2 kbar.

3. Ultrasonics

From our calculated Θ_D and measured longitudinal ultrasonic velocity u_l in solid helium at 75.22 K, we estimated the ultrasonic transverse velocity, u_t , from the relationship

$$\Theta_D = \frac{\hbar}{k} \left(\frac{6\pi^2 N}{V_s} \right)^{1/3} \left[\frac{1}{3} \left(\frac{1}{u_l^3} + \frac{2}{u_t^3} \right) \right]^{-1/3} \quad (18)$$

where \hbar , k , and N have their usual meanings and the reasonable assumption is made that ccp helium is isotropic. The result at $T_m = 75.22$ K is given in Table I.

Using similar approximations, we estimated the adiabatic compressibility coefficient for solid ^4He from

$$\chi_s = V_s [M(u_l^2 - \frac{4}{3}u_t^2)]^{-1} \quad (19)$$

and the adiabatic Poisson ratio from

$$\sigma_s = \frac{1}{2} [(u_l/u_t)^2 - 2] [(u_l/u_t)^2 - 1]^{-1} \quad (20)$$

and present the results at $T_m = 75.22$ K in Table I.

D. Melting process

1. Entropy change

We computed the entropy change on melting, ΔS_m , from the Clapeyron relation using Eqs. (8) and (9). The result, given as the dimensionless quantity

$$\Delta S_m/R = 0.901 (P_m + 0.008)^{0.3569} \times (P_m + 0.160)^{-0.3569} \quad (21)$$

is shown as the solid line in Fig. 8. It is probably fortuitous that the two exponents in Eq. (21) have identical absolute values. At $P_m = 0.1$ kbar, Eq. (21) gives $\Delta S_m/R = 0.66$ compared to the Grilly and Mills¹⁰ value of 0.68. For $P_m > 5$ kbar, Eq. (21) can be approximated by $\Delta S_m/R = 0.901$ with an error of less than 1%. In this region the fluid-solid entropy difference is almost independent of melting pressure and reaches a limiting value of $\ln 2.46$. We observed earlier that for hydrogen²⁹ the melting entropy goes through a minimum at $P_m = 1.9$ kbar and then rises

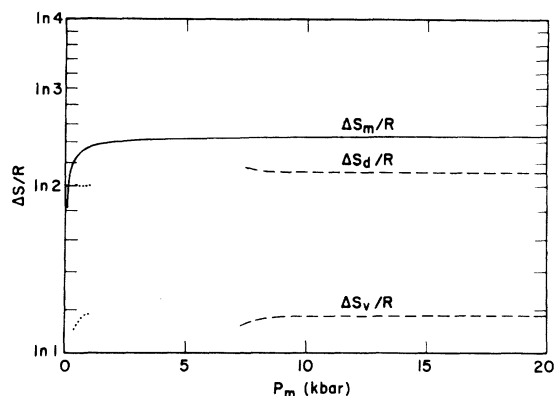


FIG. 8. Melting entropy $\Delta S_m/R$ of ${}^4\text{He}$ showing contributions from entropy of disorder $\Delta S_d/R$ and entropy of volume change $\Delta S_v/R$. Solid line, Eq. (19); dashed lines, calculated from Eqs. (7) and (19)–(21), as discussed in text; dotted lines, calculated from McCarty, Ref. 2.

slowly with pressure, whereas for argon and nitrogen $\Delta S_m/R$ falls continuously with increasing P_m . The absolute entropy of solid helium at melting can be computed from the fluid entropy by applying Eq. (21).

2. Molecular disordering

Along the melting curve up to $T_m = 15$ K ($P_m = 1.1$ kbar), fluid helium is in equilibrium with hcp solid, except for a narrow crescent-shaped band between 1.45 and 1.78 K where the bcc form exists. Above 15 K the fluid region is bounded by a ccp phase. In an attempt to study the ccp-fluid transition in ${}^4\text{He}$, we carried out an analysis similar to those previously reported for nitrogen,²⁶ argon,²⁶ and hydrogen²⁹ in which the melting entropy was broken down into two terms, namely,

$$\Delta S_m = \Delta S_v + \Delta S_d, \quad (22)$$

where ΔS_v is the entropy change caused only by the volume expansion on melting and ΔS_d is the residual entropy change due mainly to disordering of the molecules. Turturro and Bianchi⁴⁶ have calculated ΔS_v for various materials from the expression

$$\Delta S_v = \int_{V_s}^{V_f} \left(\frac{\partial P}{\partial T} \right)_V^{T_m} dV, \quad (23)$$

where $(\partial P/\partial T)_V^{T_m}$ is the isochoric pressure factor evaluated at T_m . The integration is carried out over the solid-fluid volume change at melting, $\Delta V_m = V_f - V_s$. We used Eqs. (7)–(9) and (23) to calculate ΔS_v . The dimensionless results $\Delta S_v/R$ and $\Delta S_d/R$ from Eq. (22) are plotted in Fig. 8 as the dashed

lines. Down to about $P_m = 7.4$ kbar ($T_m = 50$ K), where Eq. (7) begins to break down, the entropy of disorder $\Delta S_d/R$ has a constant value of $0.75 = \ln 2.1$, indicating that the uncertainty of locating a helium atom in the fluid structure is only 2.1 times greater than on the ccp lattice at melting. Shown also in Fig. 8 as the dotted segments are similar calculations using McCarty's data below 1 kbar. This portion of the melting line is bounded by hcp solid, from which the entropy of disorder appears to be $\ln 2.0$. We had carried out an earlier analysis on monatomic argon²⁶ and found values of $\Delta S_d/R$ between $\ln 1.8$ and $\ln 1.9$. For diatomic hydrogen²⁹ our calculated values of $\Delta S_d/R$ were between $\ln 2.0$ and $\ln 2.2$, and for diatomic nitrogen²⁶ the entropy of disorder was $\ln 1.7$. The value calculated by Hoover *et al.*⁴⁷ for a soft-sphere model is $\ln 1.9$.

Stishov *et al.*⁴⁸ attempted to extract the entropy of disorder from the melting entropy of argon and sodium by plotting $\Delta S_m/R$ against $\Delta V_m/V_s$. They found that as $(\Delta V_m/V_s) \rightarrow 0$, $(\Delta S_m/R) \rightarrow \ln 2.0$, which they interpreted as the entropy of disorder. Figure 9 shows similar plots of the materials we have studied. In all cases $\Delta V_m/V_s$ decreases with increasing P_m . The experimental regions are indicated by the solid curves with extrapolations shown by the dashed lines. Our empirical melting formulas exhibit the following behavior: for argon and nitrogen, $\Delta S_m/R$ decreases with pressure toward zero at infinite P_m ; for hydrogen, $\Delta S_m/R$ first decreases slightly, then reverses direction and goes to infinity with P_m ; and for helium, $\Delta S_m/R$ increases, but approaches a constant value at infinitely high pressure. It does not appear that meaningful extrapolations can be made from the curves in Fig. 9.

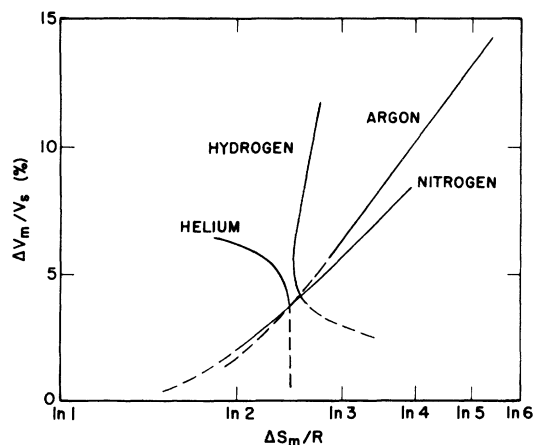


FIG. 9. Relative volume change vs entropy change on melting. Argon and nitrogen, earlier work, Ref. 26; hydrogen, earlier work, Ref. 29; helium, present work; solid lines, experimental range; dashed lines, extrapolated melting equations.

V. CONCLUSIONS

We measured 670 sets of P , V , T , and ultrasonic velocity u in fluid ^4He over the range $75 < T < 300$ K and $2 < P < 20$ kbar and fitted the data to a Benedict-type equation of state (EOS) from which we calculated various thermodynamic properties. The present values of molar volume and ultrasonic velocity with estimated errors 0.3 and 0.4%, respectively, are in generally good agreement with those reported by other workers near room temperature at pressures up to 10 kbar. Our EOS can be extrapolated down to 50 K and 1 kbar to give values of V and u that deviate by only a few percent from accepted literature values.

We made melting-curve determinations up to 20 kbar and combined our P_m, T_m points with the lower-pressure data of others to evaluate parameters in a Simon-type melting equation. Corresponding values of the volume change on melting were measured, making it possible to derive the molar volume of solid ^4He along the melting curve. Our solid volumes

are consistent with earlier values measured up to 20 kbar at 4 K. An experimental determination of the ultrasonic longitudinal velocity in solid helium was made at 14 kbar and 75 K.

We find that the Lindemann melting equation provides a good description of the melting process in ^4He . Using a Debye model, we obtained reasonable estimates of the ultrasonic transverse velocity, adiabatic compressibility coefficient, and adiabatic Poisson ratio for solid helium at 14 kbar and 75 K. Analysis of the entropy change on melting shows that an entropy of about $\ln 2$ may be associated with disordering of the atoms during melting.

ACKNOWLEDGMENTS

We thank L. C. Schmidt who built the apparatus and helped with the measurements. This work was performed under the auspices of the U.S. DOE and was supported in part by the Division of Materials Sciences of the Division of Basic Energy Sciences.

-
- ¹G. M. Wilson, R. G. Clark, and F. L. Hyman, *Ind. Eng. Chem.* **60**, 58 (1965).
- ²R. D. McCarty, *Natl. Bur. Stand. (U.S.) Tech. Note* 631 (1973).
- ³A. V. Bilevich and L. L. Pitaevskaya, *Zhr. Fiz. Khim.* **45**, 2907 (1971) [*Russ. J. Phys. Chem.* **45**, 1644 (1971)].
- ⁴L. L. Pitaevskaya and A. V. Bilevich, *Zhr. Fiz. Khim.* **44**, 1594 (1970) [*Russ. J. Phys. Chem.* **44**, 897 (1970)].
- ⁵L. F. Vereshchagin, N. A. Yuzefovich, and A. V. Chelovskii, *Dokl. Akad. Nauk (USSR)* **144**, 1272 (1962) [*Sov. Phys. Dokl.* **7**, 541 (1962)].
- ⁶T. Nishitake and Y. Hanayama, in *Proceedings of the 4th International Conference on High Pressure, Kyoto, 1964*, edited by J. Osugi (Physico-Chemical Society Japan, Kyoto, 1975), p. 534.
- ⁷D. S. Tsiklis, V. Ya. Maslennikova, and S. Ya. Gluvka, *Dokl. Akad. Nauk (USSR)* **216**, 769 (1974) [*Sov. Phys. Dokl.* **19**, 351 (1974)].
- ⁸P. W. Bridgman, *Proc. Natl. Acad. Sci. U.S.A.* **9**, 370 (1923).
- ⁹P. W. Bridgman, *Proc. Am. Acad. Arts Sci.* **59**, 173 (1924).
- ¹⁰E. R. Grilly and R. L. Mills, *Ann. Phys. (NY)* **8**, 1 (1959).
- ¹¹R. K. Crawford and W. B. Daniels, *J. Chem. Phys.* **55**, 5651 (1971).
- ¹²D. W. J. Langer, *J. Phys. Chem. Solids* **21**, 122 (1961).
- ¹³J. P. Pinceaux and J. M. Besson, in 7th International High Pressure AIRAPT Conference, Le Creusot, France, edited by B. Vodar (Pergamon, London, to be published).
- ¹⁴A. F. Schuch and R. L. Mills, in *Advances in Cryogenic Engineering*, edited by K. D. Timmerhaus (Plenum, New York, 1962), Vol. 7, p. 311.
- ¹⁵J. G. Daunt, A. F. Schuch, and R. L. Mills, *Phys. Today* **17**, 50 (1964).
- ¹⁶J. W. Stewart, *J. Phys. Chem. Solids* **1**, 146 (1956).
- ¹⁷J. W. Stewart, *Phys. Rev.* **129**, 1950 (1963).
- ¹⁸I. L. Spain and S. Segall, *Cryogenics* **11**, 26 (1971).
- ¹⁹H. Suzuki, *J. Phys. Soc. Jpn.* **42**, 1865 (1977).
- ²⁰D. J. Sanders, H. Kwun, A. Hikata, and C. Elbaum, *Phys. Rev. Lett.* **39**, 815 (1977).
- ²¹R. L. Mills, D. H. Liebenberg, J. C. Bronson, L. C. Schmidt, and D. Schiferl, Los Alamos Scientific Laboratory disclosure work sheet S-50,629 (1978) (unpublished).
- ²²D. H. Liebenberg, *Phys. Lett. A* **73**, 74 (1979).
- ²³D. H. Liebenberg, R. L. Mills, and J. C. Bronson, in 7th International High Pressure AIRAPT Conference, Le Creusot, France, edited by B. Vodar (Pergamon, London, to be published).
- ²⁴D. H. Liebenberg, R. L. Mills, and J. C. Bronson, *J. Appl. Phys.* **45**, 741 (1974).
- ²⁵R. L. Mills, D. H. Liebenberg, and J. C. Bronson, *J. Chem. Phys.* **63**, 1198 (1975).
- ²⁶R. L. Mills, D. H. Liebenberg, and J. C. Bronson, *J. Chem. Phys.* **63**, 4026 (1975).
- ²⁷R. L. Mills, D. H. Liebenberg, J. C. Bronson, and L. C. Schmidt, *J. Chem. Phys.* **66**, 3076 (1977).
- ²⁸R. L. Mills, D. H. Liebenberg, and J. C. Bronson, *J. Chem. Phys.* **68**, 2663 (1978).
- ²⁹D. H. Liebenberg, R. L. Mills, and J. C. Bronson, *Phys. Rev. B* **18**, 4526 (1978).
- ³⁰R. Wiebe, V. L. Gaddy, and C. H. Heins, Jr., *J. Am. Chem. Soc.* **53**, 1721 (1931).
- ³¹T. C. Biggs and A. R. Howard, U. S. Bur. Mines Report No. RI-7639 (1972) (unpublished).
- ³²A listing of the data is available from the authors as Report No. LA-8249-MS (1980) (unpublished).
- ³³D. H. Liebenberg, R. L. Mills, and J. C. Bronson, in *High Pressure Science and Technology*, edited by K. D. Timmerhaus and M. S. Barber (Plenum, New York, 1979), Vol. 1, p. 395.

- ³⁴M. Benedict, *J. Am. Chem. Soc.* 59, 2233 (1937).
- ³⁵G. J. Piermarini, S. Block, J. D. Barnett, and R. A. Forman, *J. Appl. Phys.* 46, 2774 (1975).
- ³⁶J. S. Dugdale and F. E. Simon, *Proc. R. Soc. London Ser. A* 218, 291 (1953).
- ³⁷R. L. Mills and A. F. Schuch, *J. Low Temp. Phys.* 16, 305 (1974).
- ³⁸J. P. Franck, *Phys. Rev. Lett.* 40, 1272 (1978).
- ³⁹B. L. Holian, W. D. Gwinn, A. C. Luntz, and B. J. Alder, *J. Chem. Phys.* 59, 5444 (1973).
- ⁴⁰A. F. Schuch and R. L. Mills, *Phys. Rev. Lett.* 8, 469 (1962).
- ⁴¹Tabular values of P , V , u , α_p , C_p , C_p/C_v , χ_T , and S , computer calculated from Eq. (7) at rounded pressures from 2 to 20 kbar along isotherms spaced 25 K apart from 75 to 300 K, are available from the authors as Report No. LA-8250-MS (1980) (unpublished).
- ⁴²F. A. Lindemann, *Z. Phys.* 11, 609 (1910).
- ⁴³J. S. Dugdale, in *Physics of High Pressures and the Condensed Phase*, edited by A. Van Itterbeek (North-Holland, Amsterdam, 1965), p. 421.
- ⁴⁴R. Wanner and J. P. Franck, *Phys. Rev. Lett.* 24, 365 (1970).
- ⁴⁵R. Wanner and H. Meyer, *Phys. Lett. A* 41, 189 (1972).
- ⁴⁶A. Turturro and U. Bianchi, *J. Chem. Phys.* 62, 1668 (1975).
- ⁴⁷W. G. Hoover, M. Ross, K. W. Johnson, D. Henderson, J. A. Barker, and B. C. Brown, *J. Chem. Phys.* 52, 4931 (1970).
- ⁴⁸S. M. Stishov, I. N. Makarenko, V. A. Ivanov, and A. M. Nikolaenko, *Phys. Lett. A* 45, 18 (1973).